SPR Screening of Metal chelating Peptides in a Hydrolysate for their Antioxidant Properties

Laetitia Canabady-Rochelle, Katalin Selmeczi, Sabrina Collin, Andreea Pasc, Laurence Muhr, Sandrine Boschi-Muller

SPR Screening of Metal chelating Peptides in a Hydrolysate for their Antioxidant Properties

Abbreviated running tittle: Screening of antioxidant metal chelating peptides using SPR

Laetitia L.S. CANABADY-ROCHELLE[1a*], Katalin SELMECZI[2], Sabrina COLLIN[3], Andreea PASC[2], Laurence MUHR[1b], and Sandrine BOSCHI-MULLER[3]

[1]Université de Lorraine, Laboratoire Réactions et Génie des Procédés (LRGP, UMR CNRS-UL 7274), [a]Equipe Bioprocédés-Biomolécules, ENSAIA, 2, avenue de la forêt de Haye, 54500 Vandoeuvre-lès-Nancy, France, [b]Equipe Sols et Eaux, ENSIC, 1 rue Grandville, 54000 Nancy, France

[2]Université de Lorraine, Laboratoire Structure et Réactivité des Systèmes Moléculaires Complexes (SRSMC, UMR CNRS-UL 7565), Faculté des Sciences et Techniques, B.P. 70239, 54506 Vandoeuvre-lès-Nancy Cedex, France

[3]Université de Lorraine, Laboratoire Ingénierie Moléculaire et Physiopathologie Articulaire (IMoPA, UMR CNRS-UL 7365), Equipe Enzymologie Moléculaire et Structurale, Campus Biologie-Santé, Faculté de Médecine, 9, avenue de la forêt de Haye, CS 50184, 54505 Vandoeuvre-lès-Nancy, France

*Corresponding author:

Laetitia CANABADY-ROCHELLE

Laetitia.canabady-rochelle@univ-lorraine.fr

Université de Lorraine, Laboratoire Réactions et Génie des Procédés (LRGP, UMR CNRS-UL 7274), Equipe Bioprocédés-Biomolécules, ENSAIA, 2, avenue de la forêt de Haye, 54500 Vandoeuvre-lès-Nancy, France

Phone number: 00 +33 (0)3. 72. 74. 38. 86.

Fax number: 00 +33 (0)3. 83. 59. 58. 24.

SPR Screening of Metal chelating Peptides in a Hydrolysate for their Antioxidant Properties

Highlights.

- Metal chelating peptides were screened in protein hydrolysates using SPR.
- An apparent affinity constant and a maximal resonance can be determined with SPR.
- K_A should represent the proportion of metal binding peptides in the hydrolysate.
- A correlation was established between SPR-determined K_A and metal chelation tests.

ABSTRACT

There is a growing need in the industrial sector (health, nutrition and cosmetic) to discover new biomolecules with various physico-chemical and bioactive properties. Various beneficial effects of peptides - notably those produced from protein hydrolysis - are reported in the literature. The antioxidant activity involves various mechanisms, among them metal chelation, studied by UV-visible spectrophotometry. In this paper, we set up an original method of screening metal chelating peptides in a hydrolysate using Surface Plasmon Resonance (SPR) for their antioxidant properties. To date, the empirical approach used several cycles of hydrolysate fractionation and bioactivity evaluation until the isolation of the pure bioactive molecule and its identification. Besides, the detection of metal-chelating peptide is not sensitive enough by spectrophotometry. For the first time, metal chelating peptides were screened in hydrolysates using SPR and a correlation was established between affinity constant determined in SPR and metal chelation capacity determined from UV-visible spectrophotometry.

1. INTRODUCTION

Food protein-derived bioactive peptides (BPs) have been reported to trigger certain physiological responses in the body, thereby influencing health positively. Those peptides have attracted high

research and consumer interest due to their huge potential in functional foods and other dietary intake to promote health. However, successful product development is limited by the fact that current manufacturing processes are either difficult to scale up, expensive, or may affect the structure-activity relations and thus the properties of those peptides.

The industrial sector (especially in health, nutrition and cosmetics) needs to discover new biomolecules presenting various physico-chemical or bioactive properties. Various beneficial effects of peptides are reported in the literature such as anti-hypertensive (Pihlanto-Leppälä, 2001; Marzak et al, 2003), anti-thrombosis (Ariyoshi, 1993), anti-carcinogeneous (Messina & Messina, 1991), opioid (Zioudrou, Streaty & Klee, 1979), anti-microbial (Broeckaert, Cammue, De Bolle, Thevissen, De Samblanx, & Osborn, 1997), or growth factor for cell culture (Franek, Hohenwarter & Katinger, 2000; Deparis et al, 2003; Farges-Haddani et al, 2006; Chabanon et al, 2008).

Peptides can be produced from enzymatic hydrolysis of proteins extracted from vegetable or animal co-products. Antioxidant peptides were already isolated from protein hydrolysate of various origins, notably from vegetable resources such as rapeseed proteins (Pan, Jiang & Pan, 2011; Zhang, Wang, Xu & Gao, 2009), chickpea (Zhang, Li, Miao & Jiang, 2011), sweet potatoes (Zhang, Mu & Sun, 2012), or lucerne (Xie, Huang, Xu, & Jin, 2008).

Antioxidant capacity is a generic term, which recovers various chemical mechanisms. On total, about twenty antioxidant tests are reported in the literature (Huang, Ou & Prior., 2005) and various complementary tests must be carried out to obtain a representative result of the whole antioxidant capacity of a given molecule.

Nevertheless, three main activities describe antioxidant power. The first one is the scavenging of various free radicals and involves either an electron transfer (ET) mechanism or a hydrogen atom transfer (HAT) mechanism. Radical scavenging activity is mainly followed by ABTS or DPPH tests, with $ABTS^{\circ+}$ or $DPPH^{\circ+}$ radicals, respectively. The second mechanism relies on the inhibition of lipid peroxidation (Farvin, Baron, Nielsen & Jacobsen, 2010), which can be followed

by oxygen consumption or MalonDiAldehyde test. Finally, metal chelation such as iron or copper ions complexation (Decker & Welch, 1990; Xie et al, 2008) is often studied as an indirect antioxidant mechanism since upon metal complexation, radical reactions in chain are inhibited and oxidation phenomena are delayed. Indeed, in living systems, the presence of transient metal ion, such as Fe^{2+} and Cu^{2+} involve the formation of Reactive Oxygen Species (ROS) as for instance, hydroxyl radicals (OH°) formed by the Fenton reaction. In addition, ferrous ions (Fe^{2+}) can catalyse the formation of hydroxyl radicals *via* the Haber-Weiss reaction, which occurs in the presence of superoxide anions. These free radicals, produced locally, can react with adjacent biomolecules and are responsible of serious damages in the biological tissue. Due to some environmental conditions (*i.e.* pollution, UV, non-equilibrated food), defence mechanisms involving antioxidants are sometimes overcome; an oxidant stress is generated, which can lead to the development of several pathologies in humans such as diabetes, rheumatoid arthritis, and cancer (Abuja & Albertini, 2001; Collins, 2005; Halliwell, 2000; Halliwell & Whiteman, 2004; Hoelzl, Bichler, Ferk, Simic, Nersesyan, & Elbling, 2005).

Yet, the low concentration of target bioactive peptides in an hydrolysate (a complex mixture of peptides sequences) and the difficulty to associate their bioactivity to one or several specific physicochemical properties constitute one of the main factors limiting their separation and their use. To valorise these bioactive peptides, one of the principal stakes is then the separation of peptides in a complex mixture, according to the desired bioactivity. The empirical approach consists in separating each hydrolysate in various fractions and in evaluating their bioactivity. These sequential steps are reiterated until reaching pure bioactive molecules identified by mass spectrometry. To date, the separation methods settled up (*i.e.* chromatography, ultrafiltration) are time-consuming. Besides, depending on the size of the peptide of interest, and its low concentration in the hydrolysate - whether present -, a detection using UV-visible spectrophotometry is often not sensitive enough.

Surface Plasmon Resonance (SPR) enables the monitoring of molecular interactions in real time. Its main advantage is the label free detection based on the phenomenon of surface plasmon resonance. While the interacting molecule (ligand) is immobilized on the surface of a sensor chip, the analyte is injected in solution and flow over the surface. The binding of the analyte to the immobilized ligand involves alteration of the refractive index at the sensor surface, which is proportional to the change in mass concentration. From sensorgram (SPR response in resonance unit plotted against time) studied at various analyte concentrations, the affinity constant of the analyte for the ligand can be determined.

Several studies reported the use of SPR for the affinity comparison of different tagged proteins to metal ions (Nieba et al, 1997; Bernaudat & Bülow, 2005; Kurzatkowska et al, 2014). Yet, Knecht et al, (2009) were the only ones to study the affinity of His-tag peptides to Ni^{2+} ions.

Hence, a direct screening of metal chelating peptides using SPR would enable to detect more rapidly their presence in a hydrolysate before launching a separation phase, that should be engaged solely in the case of positive bioactivity screening. To the author's knowledge, SPR has never been used as a screening method of metal chelating peptides related to their antioxidant capacities.

The aim of this study is to propose a new proof-of-methodology on a screening procedure of metal chelating peptides in hydrolysates for their antioxidant properties. Such approach uses SPR with a M^{2+}-NTA sensor chip. The main advantage of such technique is based on the higher sensitivity and label free detection of SPR detector as compared to classical UV-Vis spectrometry. Thanks to this methodology, the most interesting sources of hydrolysates in terms of metal chelating peptides could be screened rapidly. Moreover, another aim of this study is to correlate affinity constant determined by SPR methodology and antioxidant chemical tests based on metal chelation using UV-visible spectrophotometry.

To overcome potential interferences of non-peptide contaminants with SPR, the SPR methodology was first set up on one hydrolysate, taken as a model, with or without purification.

127 Once the methodology validated, screening was carried out on raw samples for further industrial
128 applications. Then, correlation was established between affinity constants and metal chelation
129 capacities determined on raw hydrolysates.

130

131 2. MATERIALS AND METHODS

132 2.1. Hydrolysates

133 2.1.1. Industrial specification

134 Peptide hydrolysates were provided from Kerry group (Ingredients and Flavours Department,
135 USA). They were obtained from various vegetable sources such as soy (*i.e.* H1510, H1512, and
136 UP Soy), wheat (H4601N) and rice proteins (H5603). The total and free amino acids composition
137 is given in the industrial specification (**Supplementary data, Table SD 1**). Besides, for each
138 hydrolysate, the global amino acid composition was presented by class of amino acids, with its
139 main characteristics in terms of total nitrogen (TN, %), protein and degree of hydrolysis
140 (**Supplementary data, Table SD 2**).

141 2.1.2. OPA quantification

142 As complex mixture of peptides, hydrolysates cannot be determined in molar concentration. To
143 compare them, peptide concentration was quantified using *ortho*-phthaldialdehyde test (OPA) and
144 expressed in mM glycine equivalent. This spectrophotometric dosage involves a reaction between
145 the N-terminal extremity of each peptide present in the mixture and OPA reagent (OPA;
146 ThermoFisher Scientific, Loughborough, UK) in the presence of *N*,*N*-dimethyl-2-mercaptoethyl-
147 ammonium (ThermoFisher Scientific). The chemical group obtained absorbs at a wavelength of
148 340 nm.

149 The OPA quantification was performed according to Frister**,** Meisel, & Schlimme (1988). The
150 OPA solution was prepared by dissolving 40 mg of OPA in 1 mL of pure methanol and 100 mg
151 of *N*,*N*-dimethyl-2-mercaptoethyl ammonium in a few milliliters of Borax buffer (sodium
152 tetraborate 100 mM, 1% w/v sodium dodecyl sulfate, pH 9.3, Sigma-Aldrich). These two
153 solutions were mixed in a 50 mL-volumetric flask, qsf Borax buffer. The molar concentration of
154 1 mg.mL^{-1} peptide hydrolysate solutions (20 µL) qsf Borax buffer was measured in 96-well plate
155 by spectrophotometry at 340 nm after 3 min incubation with stirring at room temperature
156 (ThermoFisher Scientific) with the OPA solution (200 µL). For each hydrolysate, molar
157 concentration (expressed in equivalent α-NH_2) was determined using a calibration curve
158 performed with glycine.

159

160 **2.1.3. Determination of total phenolics**

161 The total content of phenolic compounds was quantified by the method of Folin-Ciocalteu
162 according to the colorimetric method described by Singleton & Rossi (1965) and adapted to a 96-
163 well microplate by Mussato, Ballesteros, Martins & Teixeira (2011). Briefly, 5 µL of an
164 hydrolysate solution (25 g.L^{-1}) were mixed with 60 µL of sodium carbonate solution at 7.5%
165 (w/v) and 15 µL of Folin-Ciocalteu reagent (1N; Sigma Aldrich). Then, 200 µL of ultrapure
166 water (18 mΩ.cm^{-1}) were added and the solutions were mixed. Samples were incubated at 60°C
167 for 5 min and cooled down at room temperature. Absorbance was measured at 700 nm using a
168 microplate reader. Calibration of this test was carried out with gallic acid standard solutions (0,
169 200, 400, 600, 1000 et 1500 mg.L^{-1}) and the blank was performed with ultrapure water. The total
170 content of phenolic compounds was expressed in mass percentage of hydrolysate powder (w/w).

171

172

2.1.4. Purification of hydrolysates

Samples were purified using Solid Phase Extraction column (CC6 polyamide column, Chromabonb PA 6 mL/1000g, Macherey-Nagel, Duren, Germany) to remove polyphenols. Purification step was adapted from Collins, Ng, Fong, Wan, & Yeung, (1998). Briefly, the column was conditioned with 2 × 5 mL of ultrapure water, removed upon centrifugation (1000 g, 1 min). Then, 5 mL of hydrolysate solution (25 $g.L^{-1}$) was deposited onto the column and percolated at atmospheric pressure. The peptide fraction was eluted with 5 mL water and the column was then successively eluted with 5 mL MeOH 50%, 5 mL of pure MeOH and several washes of 0.1 M NaOH. The peptide fraction was then lyophilized and frozen until analysis.

2.2. Metal chelation tests

The antioxidant capacity determined by Cu^{2+} chelation was measured by spectrophotometry using murexide as colored indicator. A mini-review on metal chelation tests used in the literature and their experimental conditions is presented in supplementary data (**Table SD3**). This test was adapted from literature (Wu, Shiau, Chen, & Chiou, 2003; Wong, Leong & Koh, 2006 and Li, Wang, Chen & Chen, 2011). Absorbance was measured at two wavelengths, 485 nm and 520 nm, for the copper-murexide complex and the murexide alone, respectively. The ratio of absorbance (A_{485}/A_{520}) was considered proportional to the free copper ion (Cu^{2+}) concentration (Barges, Cravotto, Gianolio & Fedeli, 2006).

This test was adapted for the microplate study to reduce the time of experiments and the volume of studied solution. EDTA (EDTA disodium salt dihydrate, Fluka Chemie, Buchs, Switzerland) and carnosine (99%, Sigma Aldrich), both studied as positive controls, were prepared in hexamine buffer (10 mM Hexamine, 10 mM KCl, pH 5) first in a range of concentration 0-40 mM to determine saturation, then in the range 0-4 mM for linearization. Peptide hydrolysates were prepared similarly in a concentration range varying between 0-40 $g.L^{-1}$, concentration then

198 expressed in mM equivalent glycine. Experiment was repeated 5 times. Each sample (EDTA,
199 carnosine and hydrolysate solutions) was directly diluted in microplate with hexamine buffer for a
200 total volume of 143 µL. Then, 143 µL of a 3 mM $CuSO_4$ solution prepared in hexamine buffer
201 and 14 µL of 1 mM murexide solution were added in each well (total volume: 300 µL). The 96-
202 well plate was incubated for 3 min at ambient temperature and absorbance measured at 485 nm
203 and 520 nm. For each sample, the Cu^{2+} chelation capacity was determined according to equation
204 (3):

205 $$Cu^{2+}\ \text{complexation}\ (\%) = \frac{[(A_{485}/A_{520})_0 - (A_{485}/A_{520})_S]}{(A_{485}/A_{520})_0} \times 100 \quad (3)$$

206

207 With $(A_{485}/A_{520})_0$ = ratio of absorbances measured in the absence of sample (negative control:
208 hexamine buffer),
209 And $(A_{485}/A_{520})_s$= ratio of absorbances measured in the presence of sample (EDTA, carnosine or
210 hydrolysate).
211 For each sample, a linearization was performed in the linear part of the curve in order to
212 determine, after calculation, the indices characterizing its capacity for Cu^{2+} chelation: the EECC
213 (EDTA Equivalent copper Chelation Capacity) or the CECC (Carnosine Equivalent copper
214 Chelation Capacity). Such indices are calculated according to equations (4) and (5):

215 $$EECC = \frac{a_S}{a_{EDTA}} \quad (4)$$

216 $$CECC = \frac{a_S}{a_{Car}} \quad (5)$$

217 With a_s= the slope of the linearization line, for hydrolysate (% of copper chelated as a function of
218 peptide concentration).
219 a_{EDTA}= the slope of the linearization line for EDTA (% of copper chelated as a function of
220 EDTA concentration).

221 a_{car}= the slope of the linearization line for carnosine (% of copper chelated as a function of
222 carnosine concentration).
223

224 2.3. Affinity constant determination

225 Binding of peptides present in hydrolysate to Ni^{2+}-NTA was analysed by Surface Plasmon
226 Resonance (SPR). The SPR measurement was performed on a Biacore X100 instrument (Biacore
227 AB, Uppsala, Sweden) equipped with NTA (nitrilotriacetic acid) sensor chips at 25°C. The
228 method was adapted according to Knecht et al (2009) with slight modification on tri-histidine
229 peptide (HHH) before the study of peptide hydrolysate.

230 The eluent buffer (PBS 1X, pH 7.4) and the dispenser buffer (PBS 1X, pH 7.4, 0.005% Tween
231 20) were filtered (0.22 µm, support membrane, low protein binding, non pyrogenic, PALL) and
232 degassed by the Biacore instrument. The PBS 1X running buffer was prepared from a 10X
233 concentrate made of 67 mM $Na_2HPO_4.2H_2O$, 12.5 mM KH_2PO_4, 150 mM NaCl with a pH value
234 of 6.65. When the 10X stock solution was diluted to 1X, the final pH of PBS 1X was of 7.4.

235 Peptide hydrolysates were dissolved at various concentrations in freshly prepared PBS 1X buffer
236 before each experiment. Loading of Ni^{2+} onto the NTA chip was performed with a $NiCl_2$
237 solution (500 µM, Biacore kit, Uppsala, Sweden) and the chip surface was regenerated with
238 imidazole (500 mM) dissolved in ultrapure water (18.2 $m\Omega.cm^{-1}$), followed by a regeneration
239 solution (10 mL buffer added with 87 µL EDTA at 50 µM).

240 All binding experiments were performed at a flow rate of 20 $\mu L.min^{-1}$, starting with a 1-min
241 injection of aqueous $NiCl_2$ solution to load the NTA chip, with a 1-min stabilisation period. A
242 NTA flow cell without Ni^{2+} was used as a reference cell. Then each studied peptide hydrolysate
243 was injected on both flow path for 270 s followed by 270 s of undisturbed dissociation time. The
244 regeneration procedure consisted of 1-min injections of imidazole (500 mM) at 20 $\mu L.min^{-1}$

followed by an extra-wash with buffer-EDTA (50 μM). Upon the second regeneration procedure, the surface was washed with SDS 0.5% v/v for 1 min at a flow rate of 40 $\mu L.min^{-1}$ followed by an extra-wash after injection with running buffer. Each regeneration and washing cycle was repeated twice. One buffer blank before and between each sample series were used for double referencing during data processing (Myszka, 1999; mentioned in: Knecht et al, 2009).

The sensorgrams obtained from the SPR experiments were processed with BIAevaluate software. The isotherms obtained were expressed in Resonance Unit (RU, corrected by the offset value) as a function of the concentration of peptide hydrolysate (expression in mM equivalent glycine according to the OPA quantification). The dissociation constants (K_D, M equivalent glycine) were determined at equilibrium by fitting the experimental data with the 1:1 binding model. The affinity constant (K_A, M^{-1} equivalent glycine) was calculated as the inverse of the dissociation constant.

3. RESULTS AND DISCUSSION

3.1. Hydrolysate characterization

3.1.1. Raw hydrolysates

Hydrolysates are composed of a mixture of peptides, whose sequences are unknown. For their comparison, peptide concentration of hydrolysates solutions (1 $mg.mL^{-1}$) were quantified using OPA test in order to express their molar concentration in mM equivalent glycine. For raw hydrolysates, peptide concentration varied between 1.23 and 1.82 mM equivalent glycine (**Table 1**).

According to their specification, industrial hydrolysates have been submitted to ultrafiltration, the method commonly used to remove polyphenols (Bornman, Gokemen and Nyhuis, 2001;

Gokmen, Acar & Karahman, 2003). Thus, raw hydrolysates were supposed to be free of polyphenols. Surprisingly, total polyphenols were quantified between 3.6% (w/w) for H1510 and H1512 hydrolysates up to 5.9% (w/w) for H5603 (**Table 1**). The fact that similar value was observed for a trypsin casein hydrolysate used as a negative control (5.3±0.2 % w/w) suggests the existence of interferences in quantification method due for example to tyrosine residues in relation with their phenol group, but the presence of residual polyphenols in hydrolysates can not be rule out.

3.1.2. Purified hydrolysates

The purification method adapted from Collins et al (1998) was carried out on polyamide resins to eliminate non-peptides contaminants such as polyphenols. After a purification step, peptide concentration of hydrolysate samples was not significantly modified on the whole as proved by OPA quantifications (**Table 1**). In the meantime, there was practically no loss of total polyphenols. Nevertheless, as observed in Collins et al (1998), a significant amount of binding was seen as a brown coloration of resin, which eluted with sodium hydroxide (result not shown). Besides, the comparison of the OPA quantification test carried out on raw hydrolysate powder ($1g.L^{-1}$) and on a powder of hydrolysate purified onto CC6 polyamide column, lyophilised and then reconstituted ($1g.L^{-1}$) showed a slight increase in peptide concentration (**see Supplementary data. Figure SD1.**).

3.2. Determination of metal chelating capacity/affinity by SPR

3.2.1. Set up of SPR method on purified H5603 hydrolysate

Validation of the SPR method has been realised on the H5603 hydrolysate as a model, and in order to overcome potential interferences, in a first approach, hydrolysate purified on CC6 polyamide column was used. The initial methodology set up on HHH peptide by Knecht *et al.*

(2009) was adapted for the study of hydrolysate. Binding to Ni^{2+}-NTA was analyzed both qualitatively and quantitatively with surface plasmon resonance (SPR) using commercially available NTA sensor chips from Biacore. Purified H5603 hydrolysate was injected at a concentration varying from 0 to 40 $g.L^{-1}$ for 4.5 min at a flow rate of 20 $\mu L.min^{-1}$ to detect the association phase, followed by a dissociation time of 4.5 min at a flow rate of 20 $\mu L.min^{-1}$. This led to a clear detection of binding signals for all tested concentrations of hydrolysate with very fast association, reaching equilibrium immediately after injection, and dissociation rates, and with an excellent reproducibility of the triplicate injections (not shown) (**Figure 1**). Association and dissociation phases were shown to occur in a dose-dependent manner, suggesting the existence of an apparent affinity of the hydrolysate (peptides) for Ni^{2+}. The hyperbolic profile of the level of binding at equilibrium as a function of the sample concentration showed a saturating behaviour, suggesting the formation of peptide–Ni^{2+} complexes.

The experimental isotherm, *i.e.* the level of binding expressed in Resonance Unit (RU) in function of hydrolysate concentration expressed in mM equivalent glycine according to the NH_2 terminal concentration quantified using OPA test, was fit to the 1:1 binding model using BIAevalution (version 2) software (**Figure 1**). It enabled to determine the value of the apparent dissociation constant (K_D), the maximal signal (R_{max}) at saturation of the Ni^{2+}-NTA chip and the offset. The offset value (expressed in RU), which represents the difference in response between the reference (no Ni^{2+}) and the sample canal (with Ni^{2+}) of the chip, was used to calculate the true maximal response (R_{maxc}). From the value of the K_D, the value of the apparent affinity constant (K_A) was calculated (**Table 2**). The lowest the K_D value, the highest the affinity of metal chelating peptides for Ni^{2+} ions. Due to heterogeneity of the hydrolysate, in terms of peptide sequences and concentration of metal chelating peptides, it may be assumed that the value of the K_A should represent the proportion of metal binding peptides within the hydrolysate, whereas the value of the R_{maxc} would be more representative of the size of the formed complexes. Thus, the results

show that metal binding capacity of a hydrolysate can be quantified on purified peptide hydrolysate using Surface Plasmon Resonance.

In an industrial perspective, for screening various hydrolysates for their metal chelating peptides, metal-chelating properties should directly be explored on raw hydrolysates. Indeed, SPR experiments were performed similarly than previously on raw H5603 hydrolysate. The fact that similar values of K_A and R_{maxc} were obtained for the purified and non-purified H5603 hydrolysate (**Figure 2, Table 2**) shows that metal binding capacity can be determined directly on raw hydrolysate using Surface Plasmon Resonance.

3.2.2. Affinity constant determination on raw hydrolysates

In order to set up a direct screening method of metal chelating peptide in complex mixture, raw hydrolysates constitute the most appropriate materials. Hence, SPR experiments were performed similarly than previously on H1510, H1512, H4601N and UP Soy raw hydrolysates.

For all hydrolysates, association and dissociation phases were shown to occur in a concentration dependent manner (Results not shown). Plots of response at equilibrium in function of hydrolysate concentration present a hyperbolic profile, whatever the hydrolysate (**Figure 2**). From the fitting of these experimental binding isotherms, values of the different parameters were obtained (**Table 2**). Considering the K_A values, the apparent affinity of raw peptide hydrolysate for Ni^{2+} ions varied according to the samples studied and evolved in the following rank: H1512 < H5603 < H4601N < UP Soy < H1510. The highest affinities were measured for the H1510 hydrolysate and then for UP Soy in comparison to the other three hydrolysates.

3.3. Metal chelation

Metal chelation tests are usually performed on hydrolysate using spectrophotometric tests. A mini-review on metal chelation tests used in the literature and their experimental conditions is presented in supplementary data (**Table SD3**). Nevertheless, according to the size of the peptides of interest, and their low concentration in the hydrolysate - whether present -, a detection using UV-visible spectrophotometry may be sometimes not sensitive enough for such application.

The test of metal chelation capacity (Cu^{2+}) was validated on EDTA and carnosine using UV-visible spectrophotometry (**Figure 3, panels A and B**) and then, tested on raw hydrolysates (**Figure 3, panels C and D**). The Cu^{2+} chelation capacity (%) was plotted as a function of molar ratio (mM carnosine or EDTA /mM $CuSO_4$) (**Figure 3, panels A and B**). Saturation was observed at 87% of Cu^{2+} chelated for EDTA and 82% for carnosine. Since EDTA is known as a really good complexing agent, the totality of Cu^{2+} is considered fully chelated for a calculation corresponding to 87% chelation capacity. For a 1:1 stoichiometry between EDTA and Cu^{2+}, the copper chelated was of 62%. For a 1:1 stoichiometry between carnosine and Cu^{2+}, the copper chelated was about 30%. In comparison of the study of Wu and co-workers (2003), these authors determined the chelating ability of a 4 mM-EDTA solution at 68% and the chelating effect of a 5 mM-carnosine solution at 32%.

The M^{2+} chelation capacities (%) were plotted as a function of the molar ratio of the hydrolysate over the metal concentration (mM equivalent glycine / mM $CuSO_4$; **Figure 3**, **panels C and D**). In **Figure 3** (panels C), a Langmuir-shaped isotherm was observed for all the hydrolysates studied with saturation at about 80% copper chelation, which fit to the totality of the copper complexed as for positive controls (EDTA and carnosine). Nevertheless, as a complex mixture of peptides, all the peptides present in the hydrolysate are not able to complex the Cu^{2+} ions. In such conditions and despite the Langmuir-shaped isotherm, we cannot be sure that the binding of metal chelating peptides with metal ions can be approximated with a 1:1 model. Then, to

367 determine, the most interesting source of hydrolysate in terms of metal chelating peptides, an
368 indice expressed in equivalent chelation capacity (ECC) was calculated, considering either EDTA
369 (EECC) or carnosine (CECC) as reference (part 2.2.), using the slope of the linear part of the
370 curve (**Table 2**). Whatever the reference was, the rank remained the same: H1510 > UP Soy >
371 H5603 > H1512 > H4601N. The variations between hydrolysates observed by UV
372 spectrophotometry is less pronounced than those observed by SPR, when we compare
373 respectively the results of metal chelation indices and the affinity constants, which seems to
374 confirm once more the interest of SPR for the screening of metal chelating peptides in
375 hydrolysates.

376 According to the literature, amino acids preferentially involved in metal chelation are known. A
377 mini-review on amino acids and their functional groups involved in metal chelation is presented
378 in supplementary data (**Table SD4**). Several amino acids are concerned especially (1) aspartic and
379 glutamic acid, through their carboxylate function, (2) histidine *via* the imidazole ring, (3) arginine
380 and lysine through the amino group, (4) cysteine with its thiol group (5) serine and threonine with
381 hydroxyl. Nevertheless, over the five studied hydrolysates, relationship between the copper
382 chelation capacity (%) and the given industrial amino acid composition cannot be stated (See
383 **SD1**. Amino acid composition given in the industrial specification (**SD2**. Global amino acid
384 composition and main characteristics of the hydrolysate).

385

386 3.4. Correlations between affinity constants and metal chelation tests

387 From the former data, the relation between the affinity constants (K_A, M^{-1}) and the copper
388 chelation indices was plotted (**Figure 4, panels A and B,** for EECC and CECC, respectively). A
389 satisfactorily correlation was observed with a R^2 value of 0.88. Hence, in addition to the
390 determination of K_A for peptide hydrolysate, SPR methodology can be used for the screening
391 method of metal chelating peptides in a protein hydrolysate with more accuracy than the classical

spectrophotometric method used to date. Nevertheless, no correlation was established between affinity constant and the amino acid content in each hydrolysate given in industrial specifications (see **supplementary data SD1 and SD2**). This could be due to the fact that the amino acid residue content is not the only factor involved upon the mechanism of complexation occurring between peptide and metal ion. Indeed, the position of one amino acid residue to another one is also important in the complexation mechanism. Hence as perspective of this work, SPR experiments will be coupled to Mass Spectrometry (SPR-MS), which could help us to establish correlations between affinity and amino acid composition in regards of the peptides sequence. Such study could be extended to model peptides of known sequence to better understand the link between affinity constant and peptide concentration.

4. CONCLUSION

Surface Plasmon Resonance is a powerful tool to screen antioxidant metal chelating peptides in hydrolysate before launching time-consuming separation. Besides, SPR can directly be used on industrial hydrolysates formerly treated by ultrafiltration without an additional step of purification. A good correlation was obtained between K_A and metal chelation capacity, when both analyses were carried out on raw industrial hydrolysates. According to the results of this study, SPR is an innovative method that can be used for screening various sources of hydrolysates in terms of metal chelating peptides and could be considered for various industrial applications such as nutraceutics or cosmetics.

Acknowledgements. This work was supported in part by CNRS, Université de Lorraine and the Fédération de Recherche 3209 CNRS-UL. The access to Biacore X100 (Service Commun de Biophysicochimie des Interactions, FR3209) was deeply appreciated. The authors would like to

416 thank Kerry group for supplying raw hydrolysates. Laetitia Canabady-Rochelle thanks Emeline
417 Boyer, Tania Djehel and Nesrin Loulou for their technical assistance.

418

References

Abuja, P., & Albertini, R. (2001). Methods for monitoring oxidative stress, lipid peroxidation and oxidation resistance of lipoproteins. *Clinica Chimica Acta, 306*, 1–17.

Ariyoshy, Y. (1993). Angiotensin-converting enzyme-inhibitors derived from food proteins. *Trends in Food Science & Technology*, 4(5), 139-144.

Barges A., Cravotto G., Gianolio E., & Fedeli F. (2006). How to determine free Gd and free ligand in solution of Gd chelates. A technical note. *Contrast Media and Molecular Imaging*, 1, 184-188.

Bernaudat F. & Bülow L. (2005). Rapid evaluation of nickel binding properties of His-tagged lactate dehydrogenases using surface plasmon resonance. *Journal of Chromatography A*, 1066, 219-224.

Borneman Z., Gokemen V., and Nyhuis H.H. (2001) Selective removal of polyphenols and brown color in apple juice using PES/PVP membranes in a single ultrafiltration process. *Separation and Purification Technology*, 22-3, 53-61.

Broeckaert W.F., Cammue B.P.A, De Bolle M.F.C, Thevissen K., De Samblanx G.W., Osborn R.W. (1997). Antimicrobial peptides from plant. *Critical Review in Plant Science*, 16(3): 297-323.

Chabanon G., Alves da Costa L., Farges B., Harscoat C., Chenu S., Goergen J.L., Marc A., Marc I., Chevalot I. (2008). Influence of the rapeseed protein hydrolysis process on CHO cell growth. *Bioresourource Technology*, 99: 7143-7151.

Collins, A. (2005). Antioxidant intervention as a route to cancer prevention. European. *Journal of Cancer, 41,* 1923–1930.

Collins R.A., Ng T.B., Fong W.P., Wan C.C. and Yeung H.W. (1998). Removal of polyphenolic compounds from aqueous plant extracts using polyamide minicolumns. *Biochemistry and Molecular Biology International,* 45(4): 791-796.

443 **Decker**, E.A. & Welch, B. (1990). Role of ferritin as a lipid oxidation catalyst in muscle food.
444 *Journal of Agricultural and Food Chemistry*, 38, 674-677.

445 **Deparis** V., Durrieu C., Schweizer M., Marc I., Goergen J.L., Chevalot I. & Marc A. (2003).
446 Promoting effect of rapesseed proteins and peptides on Sf9 insect cell growth. *Cytotechnology*,
447 42:75-85.

448 **Farges-Haddani** B., B. Tessier, S. Chenu, **I. Chevalot**, **C. Harscoat**, I. Marc, J.L. Goergen, &
449 A. Marc. (2006). Peptides fractions of rapeseed hydrolysates as an alternative to animal
450 proteins in CHO cell culture media. *Process Biochemistry*, 41: 2297-2304.

451 **Farvin** K.H.S., Baron C.P., Nielsen N.S. & Jacobsen C. (2010). Antioxidant activity of yoghurt
452 peptides: Part 1-in vitro assays and evaluation in w3 enriched milk. *Food Chemistry*, 123: 1081-
453 1089.

454 **Franek** F., Hohenwarter O., & Katinger H. (2000). Plant protein hydrolysates: Preparation of
455 defined peptide fractions promoting growth and production in animal cells cultures.
456 *Biotechnoogy. Progress*, Sept-Oct,16(5): 688-692.

457 **Frister,** H., Meisel, H., & Schlimme E. (1988). OPA method modified by use of N,N-dimethyl-
458 2-mercaptoethylammonium chloride as thiol component. *Fresenius' Journal of Analytical*
459 *Chemistry*, 330, 631-633.

460 **Gokmen** V., Acar J., and Karahman N. (2003) Influence of conventional clarification and
461 ultrafiltration on the phenolic composition of golden delicious apple juice. *Journal of Food*
462 *Quality*, 26, 257-266.

463 **Halliwell**, B., & Whiteman, M. (2004). Measuring reactive species and oxidative damage in vivo
464 and in cell culture: How should you do it and what do the results mean? *British Journal of*
465 *Pharmacology*, 142, 231–255.

466 **Halliwell**, B. (2000). Lipid peroxidation, antioxidants and cardiovascular disease: How should we
467 move forward? *Cardiovascular Research*, *47*, 410–418.

468 **Hoelzl**, C., Bichler, J., Ferk, F., Simic, T., Nersesyan, A., & Elbling, L. (2005). Methods for the
469 detection of antioxidants which prevent age related diseases: A critical review with particular
470 emphasis on human intervention studies. *Journal of Physiology and Pharmacology, 56,* 49–64.

471 **Huang** D., Ou, B., & Prior R.L., (2005). The chemistry behind antioxidant capacity assay. *Journal*
472 *of Agricultural and Food Chemistry, 53,* 1841-1856.

473 **Knecht** S., Ricklin D., Eberle A.N. & Ernst B. (2009). Oligohis-Tags: Mechanisms of
474 Binding to Ni^{2+}-NTA Surfaces. *Journal of Molecular Recognition*, 22: 270–279.

475 **Kurzatkowska** K., Mielecki M., Grzelak K., Verwilst P., Dehaen W., Radecki J., Radecka H.
476 (2014). Immobilization of His-tagged kinase JAK2 onto the surface of a plasmon resonance
477 gold disc modified with different copper (II) complexes. *Talanta.* 2014 Dec; 130:336-41.

478 **Li** X., Wang X., Chen D. & Chen S. (2011). Antioxidant activity and mechanism of
479 protocatechuic acid in vitro. *Functional Foods in Health and disease*, 7: 232-244.

480 **Marczak** E.D., Usui H., Fujita H., Yang Y., Yokoo M., Lipkowski A.W., & Yoshikawa M.
481 (2003). New antihypertensive peptides isolated from rapeseed. *Peptides*, 24: 791-798.

482 **Messina** J., V. & Messina. (1991). Increasing use of soyfoods and their potential role in cancer
483 prevention. *Journal of the American Dietic Association*, 91(7): 836-840.

484 **Myszka** DG. (1999). Survey of the 1998 optical biosensor literature. *Journal of Molecular*
485 *Recognition*, 12: 390–408.

486 **Mussato** I., L.F. Ballesteros, S. Martins & J.A. Teixeira. (2011). Extraction of antioxidant
487 phenolic compounds from spent coffe grounds. *Separation and Purification Technology.* 83, 173-179.

488 **Nieba** L., Nieba-Axsmann S.E., Persson A., Hamalainen M., Edebratt F., Hansson A., Lidholm
489 J., Magnusson K., Karlsson A.F., & Pluckthun A. (1997). Biacore analysis of Histidine-
490 tagged proteins using a chelating NTA sensor chip. *Analytical Biochemistry*, 252: 217-228.

491 **Singleton** V.L., J.A. & Rossi Jr. (1965). Colorimetry of total phenolics with phosphomolybdic-
492 phosphotungstic acid reagents, *American Journal of Enology and Viticulture.* 16, 144–158.

493 **Pan** M., Jiang T.S., & Pan J.L. (2011). Antioxidant Activities of Rapeseed Protein Hydrolysates.
494 *Food and Bioprocess Technology,* 4: 1144–1152.

495 **Pihlanto-Leppalä, A.**. (2001). Bioactive peptides derived from whey proteins: opioid and ACE-
496 inhibitory peptides. *Trends in Food Science and Technology,* 11(9-10): 347-356.

497 **Wong** S.-P., Leong, L. P. & Koh J.H.W. (2006). Antioxidant activities if aqueous extracts if
498 selected plants. *Food Chemistry*, 99, 775-783.

499 **Wu** H-C., Shiau C-Y., Chen H-M. & Chiou T-K. (2003) Antioxidant Activities of Carnosine,
500 Anserine, Some Free Amino Acids and Their Combination. *Journal of Food and Drug*
501 *Analysis,* 11 (2): 148-153.

502 **Xie** Z., Huang J., Xu X., & Jin Z. Antioxidant activity of peptides isolated from alfafa leaf protein
503 hydrolysate, (2008) *Food Chemistry* 111: 370-376.

504 **Zhang** S. B., Wang Z., Xu S. Y. & Gao X.F. (2009). Purification and characterization of a radical
505 scavenging peptide from rapeseed protein hydrolysates, *Journal of American Oil Chemistry*
506 *Society*, 86: 959-966.

507 **Zhang** T., Li Y., Miao M., & Jiang B. (2011). Purification and characterisation of a new
508 antioxidant peptide from chickpea (*Cicer aretium L.*) protein hydrolysates, *Food Chemistry*,
509 128: 28-33.

510 **Zhang**, Mu & Sun. (2012). Sweet potato protein hydrolysates: antioxidant activity and protective
511 effects on oxidative DNA damage, *International Journal of Food Science and Technology*, 47: 2304-
512 2310.

513 **Zioudrou** C., Streaty R.A., & Klee W.A. (1979) Opioid peptides derived from food proteins.
514 *Journal of Biological Chemistry*, 10, 254 (7): 2446-2449.

515

List of Tables and Figures

Table 1. Characterization of hydrolysates: peptide concentration expressed in equivalent glycine, total polyphenol quantification (in mass percentage, w GAE/w hydrolysate powder; GAE: Gallic Acid Equivalent), and respective yields.

	Peptide concentration (mM equivalent glycine)		Total polyphenol quantification in mass % (w/w)		Yields in fraction collected after purification	
Hydrolysate	**Raw hydrolysate**	**Purified hydrolysate**	**Raw hydrolysate**	**Purified hydrolysate**	**Peptide - OPA quantification**	**Polyphenol (Folin-ciocalteu quantification)**
H1510	1.23	1.29	3.6 ±0.2	3.7 ±0.2	105	103
H1512	1.82	1.92	3.6 ±0.2	3.6 ±0.4	99	99
H4601N	1.38	1.74	4.6 ±0.3	4.1 ±0.2	107	87
H5603	1.50	1.74	5.9 ±0.2	5.5 ±0.4	101	93
UP Soy	1.46	1.52	4.9 ±0.3	4.2 ±0.0	101	86
Hcasein			5.3 ±0.2	4.1 ±0.3	104	82

526 **Table 2.** Dissociation (K_D, mM), Affinity constants (K_A, mM^{-1}), R_{maxc} determined by SPR and
527 metal chelation capacity determined by spectrophotometry. EDTA (EECC) and Carnosine
528 Equivalent Chelation Capacity (CECC) determined for Copper (II) on raw hydrolysate.

Nature of the hydrolysate	Sample	K_D (mM eq. Glycine)	K_A (mM^{-1} eq. glycine)	R_{maxc} (RU)	Slope of the tangent at the origin (Chelated Cu^{2+} % / molar ratio)	EECC for copper (II)	CECC for copper (II)
Purified	H5603	0.90	1.11	319			
	H1510	0.10	9.92	60	91.9	2.23	3.21
	H1512	2.58	0.39	125	56.5	1.37	1.97
Raw	H4601N	0.78	1.29	64	51.5	1.25	1.80
	H5603	1.04	0.96	418	59.4	1.44	2.07
	UP Soy	0.14	6.95	129	69.8	1.70	2.44
EDTA					41.2	1	/
Carnosine					28.6	/	1

529

530

531 **Figure 1.** Sensorgram (down graph) and corresponding sorption isotherm (top graph) of purified

532 (A) and raw (B) H5603 hydrolysate.

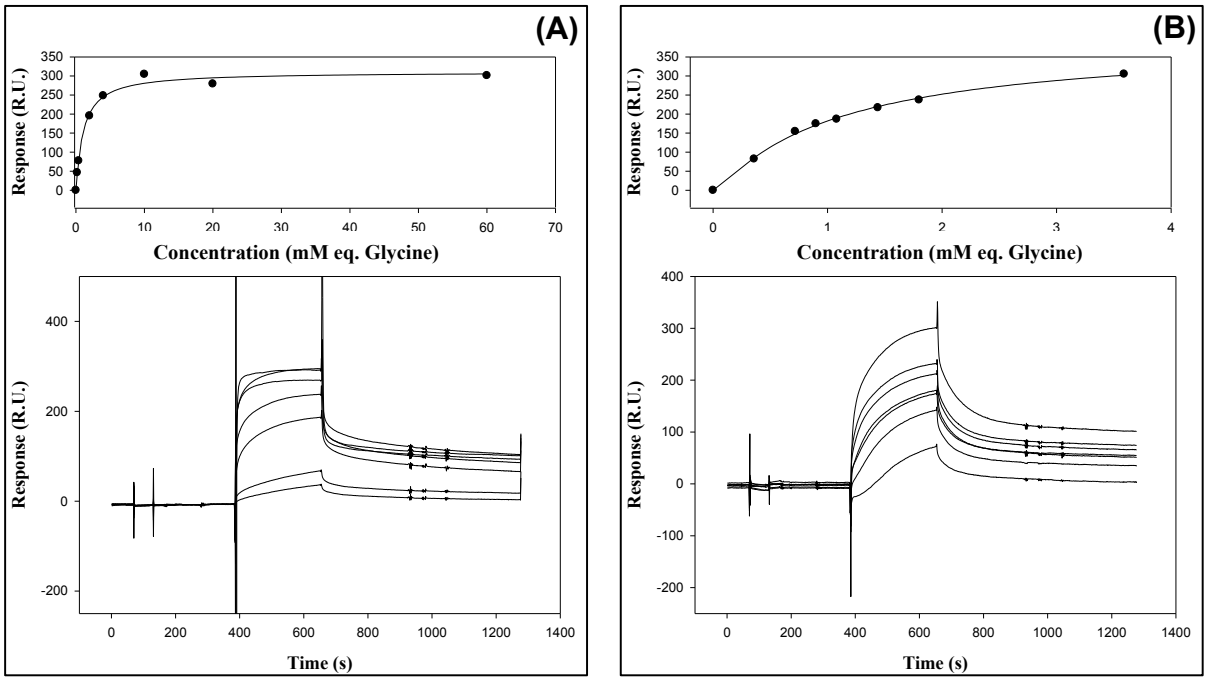

533
534

Figure 2. Sorption isotherms enabling the determination of the dissociation constant for various raw hydrolysates. Data corrected by the offset and hydrolysate concentration expressed in mM equivalent glycine. Experimental points and their respective fits.

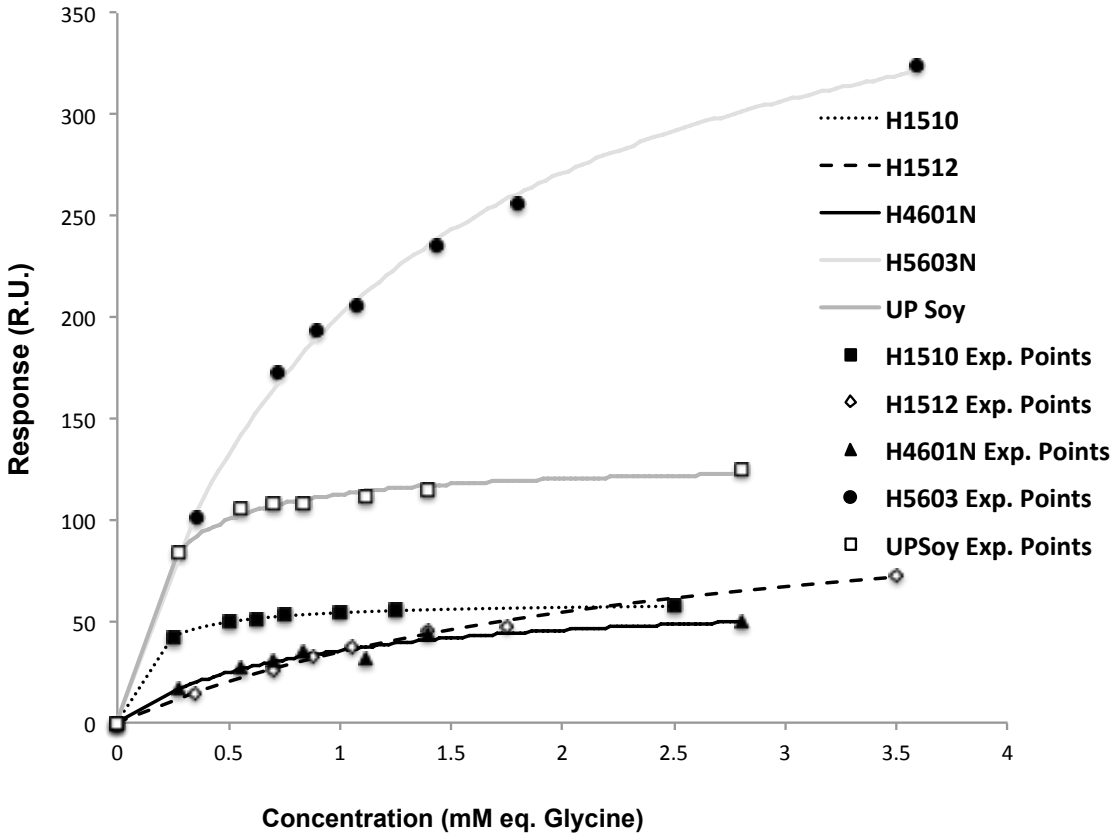

Figure 3. Results of metal chelation obtained by spectrophotometry. Panels A and B for EDTA and carnosine. Panels C and D for hydrolysates.

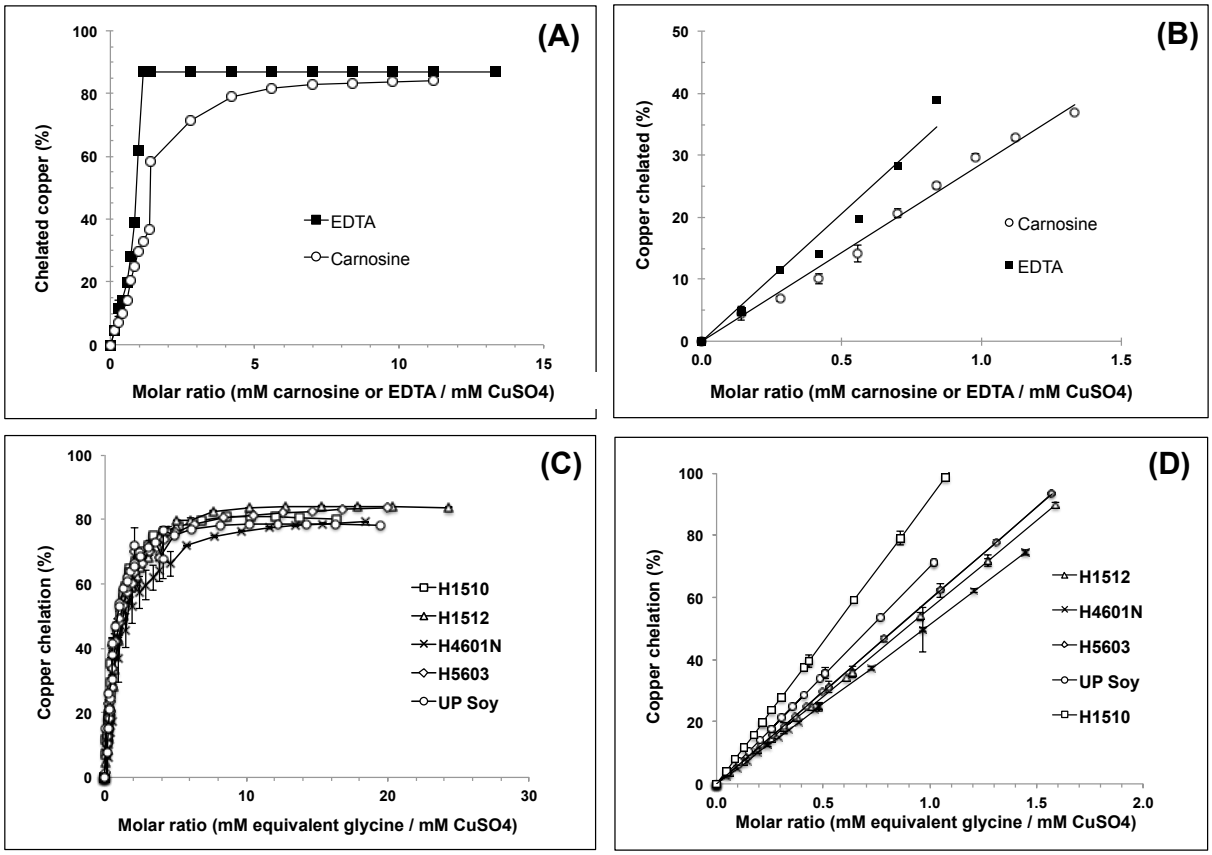

Figure 4. Correlation between affinity constant (K_A, M^{-1} equivalent glycine) and copper (II) chelating activity in raw hydrolysate. (A) Metal chelation expressed as EECC. (B). Metal chelation expressed as CECC.

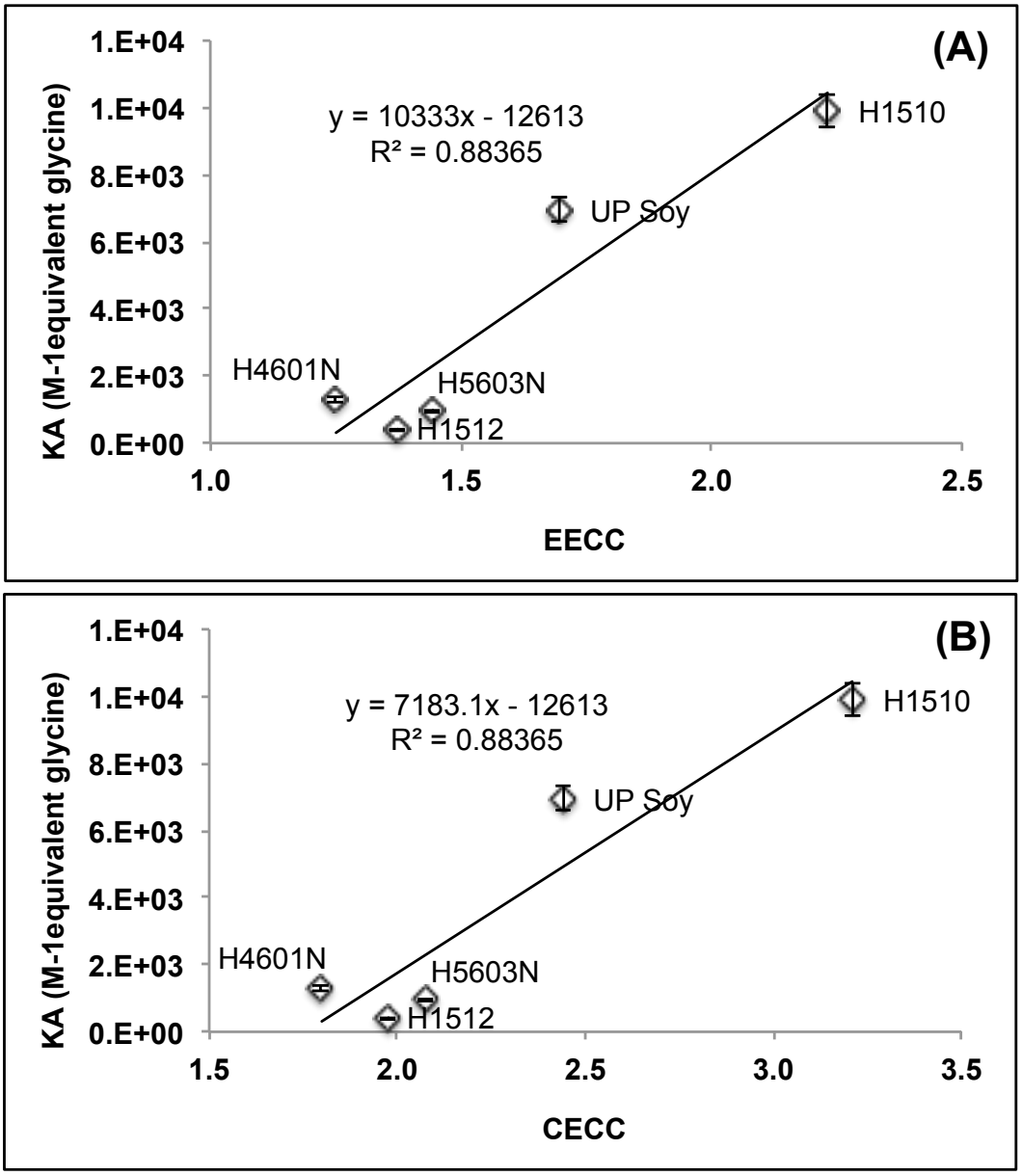

Supplementary Data

Table SD1. Amino acid composition given in the industrial specification.

Characteristics of samples		1510	1512	4610N	5603	UP Soy
Total AA (mg/g)	Ala	26.0	25.0	21.0	48.0	19.0
	Arg	41.0	37.0	27.0	72.0	30.0
	Asn					0.0
	Asp	73.0	66.0	24.0		51.0
	Cys	4.0	3.0	11.0	8.0	0.0
	Gln					
	Glu	122.0	112.0	319.0		79.0
	Gly	25.0	24.0	27.0	37.0	13.0
	His	14.0	13.0	15.0	20.0	9.0
	Ile	23.0	22.0	32.0	34.0	19.0
	Leu	40.0	38.0	57.0	66.0	30.0
	Lys	38.0	32.0	11.0	35.0	33.0
	Met	7.0	7.0	12.0	15.0	2.0
	Phe	26.0	24.0	46.0	43.0	20.0
	Pro	28.0	27.0	115.0	38.0	39.0
	Ser	31.0	29.0	38.0	44.0	21.0
	Thr	24.0	22.0	21.0	31.0	17.0
	Trp					
	Tyr	21.0	20.0	29.0	43.0	17.0
	Val	25.0	24.0	32.0	49.0	19.0
Free AA (mg/g)	Ala	2.6	3.8	1.9	0.6	5.6
	Arg	9.2	9.8	8.6	1.0	9.9
	Asn		2.4	1.8	0.9	4.0
	Asp	2.1	3.1	0.7	0.4	5.1
	Cys				2.9	0.1
	Gln	3.5	0.2	1.2	0.4	
	Glu		5.2	0.4	2.9	6.9
	Gly	2.5	3.6	1.0	0.1	1.1
	His	1.4	1.3	3.2	0.1	2.6
	Ile	0.5	1.6	4.8	0.2	4.8
	Leu	6.3	11.0	10.7	1.9	13.9
	Lys	4.6	6.4	2.3	0.6	10.8
	Met	0.9	1.7	2.0	0.2	1.3
	Phe	2.7	4.4	4.9	1.4	7.7
	Pro		0.3	0.5	0.3	0.6
	Ser	4.0	4.9	3.9	1.1	5.4
	Thr	1.7	2.2	5.7	0.3	4.8
	Trp	1.5	2.5	3.0		4.5
	Tyr	1.1	1.6	1.3	0.1	1.7
	Val	1.0	2.0	5.0	0.1	5.0

Table SD2. Global composition in amino acids (AA; mg/g) by class and main characteristics of the studied hydrolysates. TN: Total Nitrogen (%). DH: ratio AN/TN x 100.

		1510	1512	4610N	5603	UP Soy
Global amino-acid (AA) composition (mg/g)						
Positively charged AA (RHK)	Total	93	82	53	127	72
	Free	15	18	14	2	23
Negatively charged AA (DE)	Total	195	178	343	0	130
	Free	2	8	1	3	12
Polar uncharged AA (STNQ)	Total	55	51	59	75	38
	Free	9	10	13	3	14
Sulfured AA (CM)	Total	11	10	23	23	2
	Free	1	2	2	3	1
Hydrophobic AA (AVILMFYW)	Total	168	160	229	298	126
	Free	17	29	34	5	45
Aromatic AA (FYW)	Total	47	44	75	86	37
	Free	5	9	9	2	14
Other parameters						
Total Nitrogen (TN, %)		9.2	8.8	14.2	12.8	8.0
DH (ratio AN/TN x100)		16-29	27.5	15.4	14-22	25-35
DH (ratio AN/TN x100), mean value		22.5	27.5	15.4	18.0	30.0

560 **Table SD3.** Mini-review on copper chelation tests carried out on peptides and on hydrolysate in

561 the literature and their experimental conditions.

	Wu et al, 2003	Saiga et al, 2003	Carasco-Castilla et al, 2012	Carasco-Castilla et al, 2012b	Guo et al, 2015	Torres-Fuentes et al, 2011	Zhang et al, 2011
Sample nature	Peptides	Hydrolysate	Hydrolysate	Hydrolysate and peptide fraction	Peptide hydrolysate	Chickpea protein hydrolysate	Hydrolysate
Range of concentration, volume sample	0.5-40 mM, 2 mL		100 μg	100 μg for hydrolysate or 50 μg for peptide	Sample, 100 μg/mL, 200 μL	n.d.	1 mL
Method adapted from	Shimada et al, 1992		Saiga et al, 2003	Saiga et al, 2003	Saiga et al, 2003	Saiga et al, 2003	Kong and Xiong, 2006
Positive control	n.d.	EDTA at 0.045%	n.d.	n.d.	CPPs***	n.d.	n.d.
Negative control (blank)	Deionized water, treated with reverse osmosis		n.d.	n.d.	Deionized ater	n.d.	n.d.
Buffer	Hexamine buffer (10 mM), KCl (10 mM)		Na acetate buffer, 50 mM, 290 μL	Na acetate buffer, 50 mM, 290 μL	Na acetate buffer, 50 mM,	Na acetate buffer, 50 mM,	Pyridine, 10%, 1 mL
pH ajusted	No		pH 6.0		pH 5.0	pH 6.0	
Copper source and concentration	$CuSO_4$, 3 mM, 2 mL	$CuSO_4$, 2 mM, 1 mL; mixed with pyridine (pH 7.0)	$CuSO_4.5H_20$, 1μg	$CuSO_4.5H_20$, 10μg	$CuSO_4$, 1 mg/mL, 20 μL	$CuSO_4$, 0.1 μg/μL, 100 μL	$CuSO_4$, 2 mM, 1 mL
Metal chelating indicator, concentration, volume	TMM*, 1 mM, 0.2 mL	PV**, 20 μL	PV**, 4 mM, 6 μL	PV**, 4 mM, 6 μL	PV**, 2 mM, 10 μL	PV**, 4 mM, 25 μL	PV** 0.1%, 20 μL
Incubation: time, temperature	3 min, RT				5 min, 37°C		
Wavelength (s)	485 nm	632 nm	632 nm	632 nm	632 nm	632 nm	632 nm
Cu^{2+} chelating ability (%)	$((A_0-A_s)/A_0)x100$		$((A_0-A_s)/A_0)x100$	$((A_0-A_s)/A_0)x100$		$(1-(A_s/A_0))x100$	$(1-(A_s/A_0))x100$
Standard curve	n.d.		n.d.	n.d.	n.d.	n.d.	n.d.
Scale	Cuvette		Microplate reader	Microplate reader	Microplate reader	n.d.	Cuvette

* TetraMethylMurexide

**Pyrocatechol Violet

CPPs: CaseinoPhosphoPeptides

n.d.: not determined

562

563

564 **Table SD4**. Amino acids and their functional group involved in metal chelation.

565

Aminoacid	Group involved	Atom involved	pK_a	pK_b	pK_R	Reference
Aspartic acid	Carboxylate	Oxygen rich group	2.09	9.82	3.86	Zacchariou and Hearn, 1996
Glutamic acid			2.19	9.67	4.25	Lv et al, 2009
						Bamdad and Chen, 2013
						Zhang et al, 2009
						Gerbino et al, 2011
Histidine	Imidazole	Nitrogen rich group	1.82	9.17	6.00	Zacchariou and Hearn, 1996
						Zoroddhu et al, 2009
						Lv et al, 2009
						Wu et al, 2003
Arginine	Amino group	Nitrogen	2.17	9.04	12.48	Farvin et al, 2010
Lysine			2.18	8.95	10.53	Zhang et al, 2009
Cystein	Thiol	Sulfur	1.71	8.33	10.78	Lv et al, 2009
Serine	Hydroxyl	Oxygen	2.21	9.15		Lv et al, 2009
Threonine			2.63	10.43		Bamdad and Chen, 2013
						Storckdieck et al, 2007
						Swain et al, 2002
						Taylor and Layrisse, 1986
Glycine	n.d.	n.d.	2.34	9.60		Wu et al, 2003
Alanine			2.35	9.69		

566

567

568 **Figure SD1.** OPA quantification test carried out on raw hydrolysate powder (1 g/L) and on
569 powder of hydrolysate purified onto CC6 polyamide column, lyophilised and reconstituted
570 (1g/L).

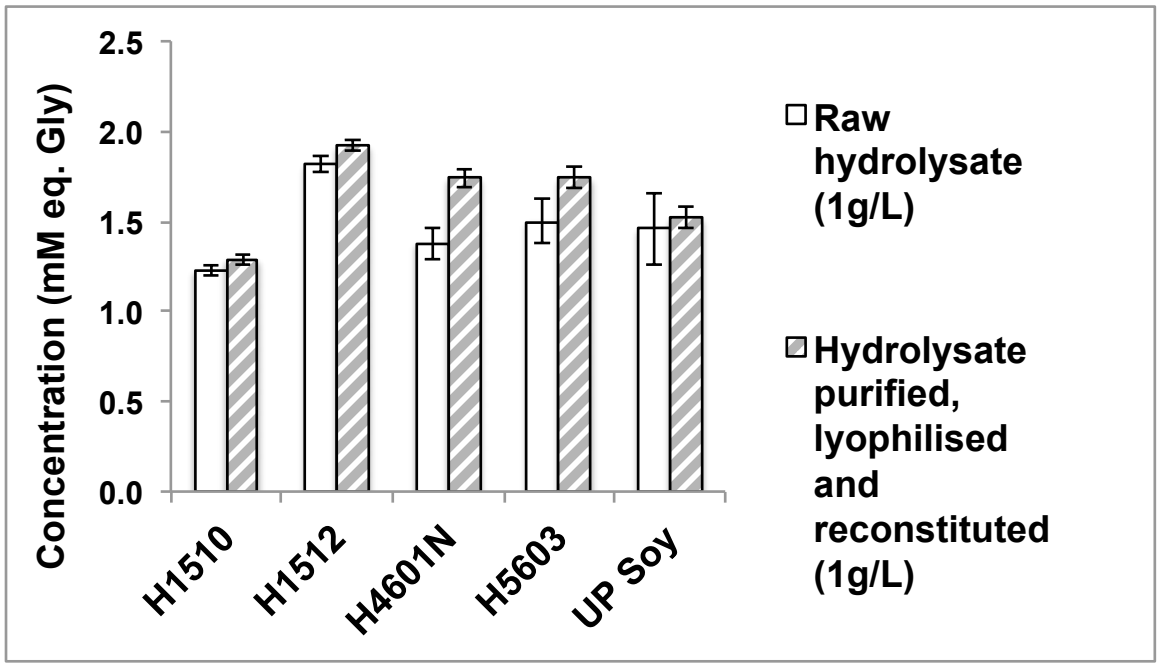

571
572
573
574
575
576
577
578
579